

Distribution of Optical and Hydrological Characteristics in the Antarctic Sound Based on the Measurements in January, 2022 in the 87th cruise of the R/V “Akademik Mstislav Keldysh”

A. A. Latushkin ¹, ✉, V. I. Ponomarev ², P. A. Salyuk ², D. I. Frey ^{1, 3},
N. A. Lipinskaya ¹, S. P. Shkorba ²

¹ Marine Hydrophysical Institute of RAS, Sevastopol, Russian Federation

² V. I. Il'ichev Pacific Oceanological Institute, Far Eastern Branch of Russian Academy of Sciences,
Vladivostok, Russian Federation

³ Shirshov Institute of Oceanology, Russian Academy of Sciences, Moscow, Russian Federation
✉ sevsalat@gmail.com

Abstract

Purpose. The purpose of the work is to study the different-scale features of distribution of the hydrooptical and hydrological characteristics in the Antarctic Sound based on the contact and satellite measurements carried out in January, 2022 in the 87th cruise of the R/V “Akademik Mstislav Keldysh”.

Methods and Results. The data of complex natural measurements performed at the oceanographic stations in the Antarctic Sound on January 27–28, 2022 in the 87th cruise of the R/V “Akademik Mstislav Keldysh” were used. Additionally, the satellite data were analyzed. Complex hydrophysical equipment permitted to obtain the vertical profiles of temperature, salinity, dissolved oxygen, chlorophyll *a* concentration, fluorescence intensity of colored dissolved organic matter, intensity of the beam attenuation coefficient at 660 nm and photosynthetically active radiation. Based on these data, the main features of mesoscale circulation within the cyclonic gyre over the deep-sea part in the southern Antarctic Sound were determined. The joint analysis of hydrooptical and hydrological characteristics, and satellite measurements in the Antarctic Sound obtained in course of the Antarctic expedition showed presence of a system of the alternating anticyclonic and cyclonic eddies in the area under study. It is also shown that in the ice drift area polluted by land soils or shelf bottom sediments, a zone of the increased turbidity arises that is related to the terrigenous suspension entering into the water during ice melting.

Conclusions. The system of the different-scales eddies and currents in the Antarctic Sound contributes to the water exchange between the upper and deep layers of the strait, as well as between the Weddell Sea water spreading to the north-northwest along the slope of the strait basin adjacent to the shelf edge of the Antarctic Peninsula and the Bransfield Strait waters spreading along the slope of the islands' shelf which is the northeastern boundary of the strait.

Keywords: Antarctic Sound, mesoscale eddies, hydrooptics, hydrology, beam attenuation coefficient, chlorophyll *a* concentration, fluorescence, dissolved organic matter, remote sensing

Acknowledgment: Study of mesoscale eddies based on natural and remote measurements was supported within the framework of state assignments MHI FNNN-2022-0001, FNNN-2021-0003, and POI No. 122110700009-1, No. 121021500054-3. Processing and analysis of hydrophysical data were supported by the RSF grant 22-77-10004.

For citation: Latushkin, A.A., Ponomarev, V.I., Salyuk, P.A., Frey, D.I., Lipinskaya, N.A. and Shkorba, S.P., 2023. Distribution of Optical and Hydrological Characteristics in the Antarctic Sound Based on the Measurements in January, 2022 in the 87th cruise of the R/V “Akademik Mstislav Keldysh”. *Physical Oceanography*, 30(1), pp. 47-61. doi:10.22449/1573-160X-2023-1-47-61

DOI: 10.22449/1573-160X-2023-1-47-61

© A. A. Latushkin, V. I. Ponomarev, P. A. Salyuk, D. I. Frey, N. A. Lipinskaya, S. P. Shkorba, 2023

© Physical Oceanography, 2023



Introduction

The Antarctic Sound, connecting the Weddell Sea with the Bransfield Strait, is located between the northeastern tip of the Antarctic Peninsula and the archipelago of islands, the largest of which is Joinville Island. The length of the strait is ~ 50 km, the maximum width reaches 19 km.

The greatest depth of the Antarctic Sound northern shelf on the boundary with the Bransfield Strait is 100 m, the depth of the strait trench on the boundary with the Weddell Sea is ~ 800–1000 m. In the central part of the Antarctic Sound there is a seamount, the top of which is at a depth of 300 m. At the southern foot of this seamount, the depth of the strait reaches an absolute maximum of ~ 1000 m in a depression that continues southward into the Weddell Sea. On other sides, the depth of the canyons at the foot of the mount does not exceed 500 m. The noted features of the rugged bottom topography, in particular the seamount, should have a significant effect on the mesoscale circulation in the strait. Moreover, stable mesoscale eddies can form not only above seamounts, but also directly above the channel of the strait. For example, chains of mesoscale eddies of opposite signs form along the axis of the strait and the slopes of the trench above the Tatar Strait of the Sea of Japan [1]. In the Drake Strait, the mesoscale eddies also form [2], as in many other straits.

The water of the Weddell Sea, rich in nutrients and phytoplankton, propagates in the Antarctic Sound along the continental slope of the Antarctic Peninsula [3], while the water of the Bransfield Strait propagates mainly in the upper layer in a southerly direction along the slope of the bottom topography near the eastern boundary of the strait – a ridge of islands, including the largest one – Joinville Island [4].

In February 2020, during the Antarctic expedition onboard R/V *Mstislav Keldysh* (79th cruise), continuous measurements of the current velocity by the vessel ADCP along the vessel's route and STD-probings on the longitudinal and transverse sections in the Antarctic Sound were performed [3]. The transverse section was located in the central part of the strait. Based on the ADCP data analysis, a characteristic cyclonic circulation in the strait (clockwise in the Southern Hemisphere) was revealed, limited from the north, east, and west by the shelf edge, from the south – by the narrowing of the depression and a decrease in the strait width. It follows from the *T*, *S* diagrams that, within this cyclonic eddy, the waters of the Weddell Sea mix with the Bransfield Strait waters [3].

It is considered that the main flux of the Weddell Sea cold waters enters the Bransfield Strait not through the Antarctic Sound, but along the bottom slopes north of D'Urville and Joinville islands [4–6]. The inflow of the Weddell Sea cold waters through the Antarctic Sound into the Bransfield Strait is hindered due to the peculiarities of the bottom topography, but occasionally occurs under favorable conditions [7, 8].

According to observational data [9–13] and the results of numerical hydrodynamic modeling [1], mesoscale [1, 9–12] and submesoscale [13] eddies form in most straits with a nonuniform bottom topography. Along the axis of the strait, alternating paths of mesoscale eddies of opposite signs are often observed [1]. A

system of mesoscale eddies was also observed in the southern part of the Drake Strait [14], in the Bransfield Strait, and in the Weddell Sea [14, 15]. It has been demonstrated that mesoscale eddies significantly affect the transport of waters of various origins, the water exchange between the shelf and the deep sea [14, 16–18] and, accordingly, the spatial distribution of hydrooptical and hydrochemical characteristics, as well as biological communities.

The purpose of this work is to study the multi-scale features of the distribution of optical and hydrological characteristics in the Antarctic Sound according to the data of contact and satellite measurements in January 2022 on the 87th cruise of R/V “Akademik Mstislav Keldysh”.

Materials and methods

As part of the expedition research program of R/V “Akademik Mstislav Keldysh” 87th cruise, on January 27–28, 2022, comprehensive *in-situ* measurements of hydrooptical and hydrological parameters were performed on two sections in the Antarctic Sound (Fig. 1). The first is a longitudinal section, located approximately along the axis of the strait, it includes 6 oceanographic stations for measuring vertical profiles of various oceanographic characteristics, performed by sounding equipment. Five stations were located directly in the Antarctic Sound, and the sixth was located in the Weddell Sea, outside the southern boundary of the strait. The second section, including 5 stations, was carried out across the strait between Joinville Island and the Antarctic Peninsula abeam Esperanza Base, which is the Argentine Antarctic research station. Similar sections in the Antarctic Sound were performed on the 79th cruise of R/V “Akademik Mstislav Keldysh” in January 2020 [3], so they can be considered the beginning of a regular series of measurements.

A joint analysis of the results of measurements of hydrooptical and hydrological characteristics on these intersecting sections makes it possible to identify the zones of ascending and descending vertical movements characteristic of mesoscale circulation and the system of currents of a larger scale during the measurement period.

The *in-situ* measurements were carried out using a complex of probing hydrological and hydrooptical equipment, which includes Idronaut, Turner C6P and Condor probing meters. Temperature (T), salinity (S), dissolved oxygen (O_2), and chlorophyll a (Chl- a) fluorescence intensity down to the bottom were measured using Idronaut probe. The Turner C6P instrument measured the fluorescence intensity of the colored dissolved organic matter (CDOM). The Condor probe was applied to determine the beam attenuation coefficient at a wavelength of 660 nm (BAC_{660}) and photosynthetically active radiation (PAR). In the red region of the spectrum, the beam attenuation coefficient is determined by the absorbing and scattering properties of the total suspended matter (TSM) and does not depend on the CDOM absorption [19]. The measurements with Turner C6P and Condor probes were carried out only on a longitudinal section and to depths not more than 250 m.

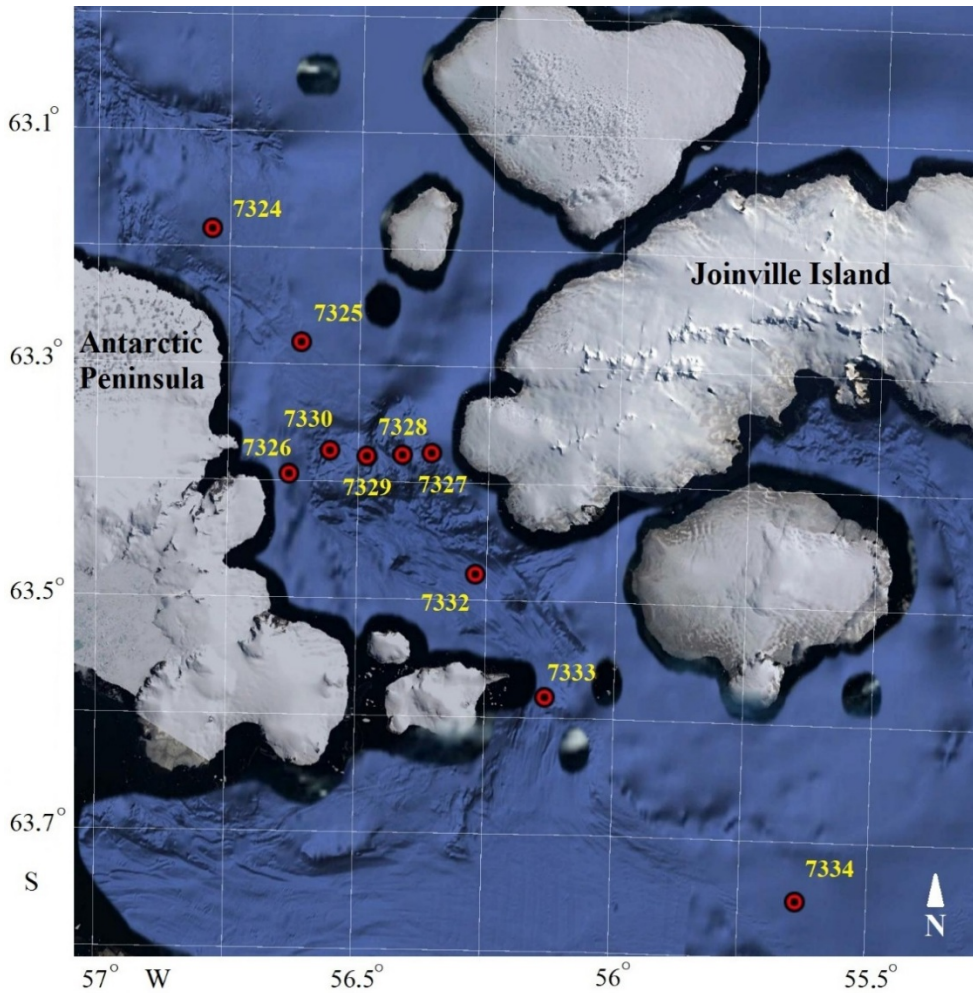


Fig. 1. Scheme of location of oceanographic stations and bottom topography in the Antarctic Sound (measurements were carried out on January 27–28, 2022)

Chl-*a* fluorescence intensities were recalculated into its mass concentrations (C_{chl-a} , $\mu\text{g/l}$) according to the dependence provided by the manufacturer of the Idronaut probe. This relationship was verified by comparison with standard determinations of C_{chl-a} performed by the extract method in the area under study. Satisfactory results were obtained: the coefficient of determination $R^2 = 0.71$, and the slope coefficient k in a straight line $y = kx$ did not differ significantly from unity at a confidence level of 0.95.

CDOM (F_{CDOM}) fluorescence intensity values are calibrated to Quinine Sulfate Units (QSU) under laboratory conditions just before the expedition. BAC_{660} was calibrated in laboratory conditions before the expedition based on the results of measurements in formazin suspension solutions with a given concentration in Formazin Turbidity Units (FTU).

Satellite measurements were used as additional information, namely:

– RGB image of the sea surface obtained from the data of OLI radiometer (pixel size ~ 30 m), installed on Landsat-8 satellite, for January 17, 2022 for the southeastern part of the Antarctic Sound and the adjacent western part of the Weddell Sea. The spatial resolution of the image is ~ 30 m. The numbers of OLI radiometer channels we used and the wavelength of maximum sensitivity are as follows: red (*R*) – No. 4 (654.5 nm), green (*G*) – No. 3 (561.5 nm), blue (*B*) – No. 2 (482 nm);

– a fragment of a high-resolution image (5–40 m) of Sentinel-1 satellite radar, obtained on February 19, 2022 at a weak wind in the area of the previous hydrologo-hydrooptical contact measurements on the transverse section and the corresponding part of the longitudinal section in the Antarctic Sound, performed on 27–28 January 2022.

These satellite measurements are selected from many others according to the quality criteria corresponding to clear weather for optical probing and light wind up to 5 m/s for radar sounding, as well as from the point of view of the shortest distance in time from the date of ship measurements. Optical and radar satellite data of high spatial resolution were applied, since they provide the most detailed analysis of eddy structures with a scale of less than 10 km [20–22].

The satellite RGB image contains information about the presence of ice fragments and icebergs, as well as other floating objects. On the radar image, in addition to ice, areas of the sea surface “smoothing” are distinguished. Such data help to identify features of multiscale circulation in the Antarctic Sound, including mesoscale eddies and currents, and to correctly interpret the results of STD and hydrooptical measurements on the transverse and longitudinal sections in the strait.

Below we provide a photograph of contaminated drifting ice in the area of station 7332, taken by the first author of the paper on January 28, 2022, which helps to correctly interpret the spatial heterogeneity of the hydrooptical probing data of the sea upper layer up to 250 m.

Results of the study

Longitudinal section. It includes 6 hydrological and hydrooptical stations located approximately along the axis of the Antarctic Sound (stations 7324, 7325, 7329, 7332, 7333, 7334), their location is demonstrated in Fig. 1. The analysis of the longitudinal section data (Fig. 2) revealed a significant difference in water masses in the northern and southern parts of the strait. The water entering the northern shelf part of the Antarctic Sound from the Bransfield Strait (stations 7324, 7325) has a higher temperature with the highest values of $\sim -0.1^\circ\text{C}$ in the upper 60-m layer (Fig. 2, *a*). This water has an increased salinity (Fig. 2, *b*), but unlike the temperature, its maximum, ~ 34.55 PSU, is located deeper – at a horizon of 150 m.

Hydrooptical characteristics at stations 7324 and 7325 have low values: C_{Chl-a} (Fig. 2, *c*) does not exceed $1 \mu\text{g/l}$, BAC_{660} (Fig. 2, *f*) – 0.35 FTU. The values of C_{Chl-a} and BAC_{660} decrease with depth. The minimum F_{CDOM} values (Fig. 2, *e*) in this area are observed in the upper mixed layer of 50 m, as in the Bransfield Strait. The depth of the photic layer (Z_{eu}) at these northern stations of the section reaches a maximum value of 85 m for the entire Antarctic Sound.

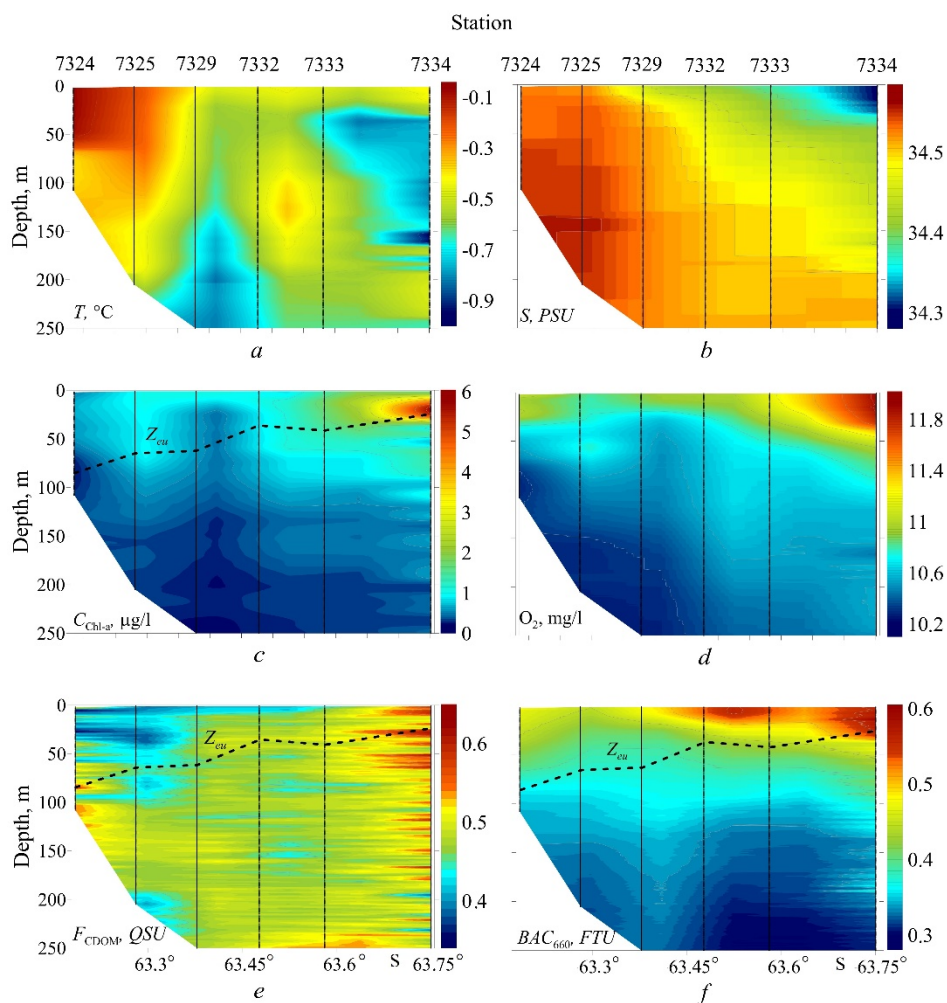


Fig. 2. Longitudinal vertical section of temperature (*a*), salinity (*b*), chlorophyll *a* concentration (*c*) and dissolved oxygen (*d*), fluorescence intensity of colored dissolved organic matter (*e*) and beam attenuation coefficient on the wavelength 660 nm (*f*). Dashed lines indicate the photic zone depth

At the same stations, a low content of O_2 was recorded (Fig. 2, *d*): in the near-surface layer, its concentration is ~ 11 mg/l, in the bottom layer, it is ~ 10 mg/l.

On sections T , C_{chl-a} , O_2 , and F_{CDOM} at station 7325, a significant deepening of the isolines of these characteristics is observed, which usually occurs during downwelling in the central part of the anticyclonic mesoscale eddy.

At stations 7332 and 7333, on the vertical temperature section in the intermediate layer of 100–200 m, a core of relatively warm water with an increased content of O_2 (Fig. 2, *d*) and low F_{CDOM} values (Fig. 2, *e*) is observed. Such features of the vertical distribution of the noted values are often traced in the central part of anticyclonic eddies [23].

At station 7332, a spot with high BAC_{660} values and, accordingly, weak penetration of PAR into the water column was revealed in the near-surface 20-meter layer. At the same time, the remaining hydrooptical characteristics remain the same

as in the surrounding waters, which may indicate the influx of suspended particles not associated with phytoplankton.

The coldest and freshest waters of the upper mixed layer with the highest O_2 content (11.2 mg/l) are observed at the southern boundary of the Antarctic Sound (station 7333, 0–20 m layer), where $T = -0.7^\circ\text{C}$, $S = 34.35$ PSU. In the adjacent area of the Weddell Sea shelf (station 7334), the temperature is approximately the same, the salinity is lower by 0.05 PSU, and the dissolved oxygen content is higher by 0.8 mg/l.

At these stations, an increase in the values of all hydrooptical characteristics was observed with maximum values at the last southern station (7334) of the longitudinal section. On the vertical profile, the maximum C_{Chl-a} (6 $\mu\text{g/l}$) is located at a depth of 20 m. The highest BAC_{660} values within the range of 0.55–0.6 FTU were observed in 0–50 m layer. The high values of C_{Chl-a} and BAC_{660} are due to the development of phytoplankton in this layer. The F_{CDOM} maximum (0.6 QSU) was obtained in 0–70 m layer. The depth of the photic layer at station 7334 was minimal and made up 24 m.

Transverse section. The differences in hydrophysical characteristics in the western and eastern regions of the strait were determined on the transverse section in the middle part of the Antarctic Sound (Fig. 3).

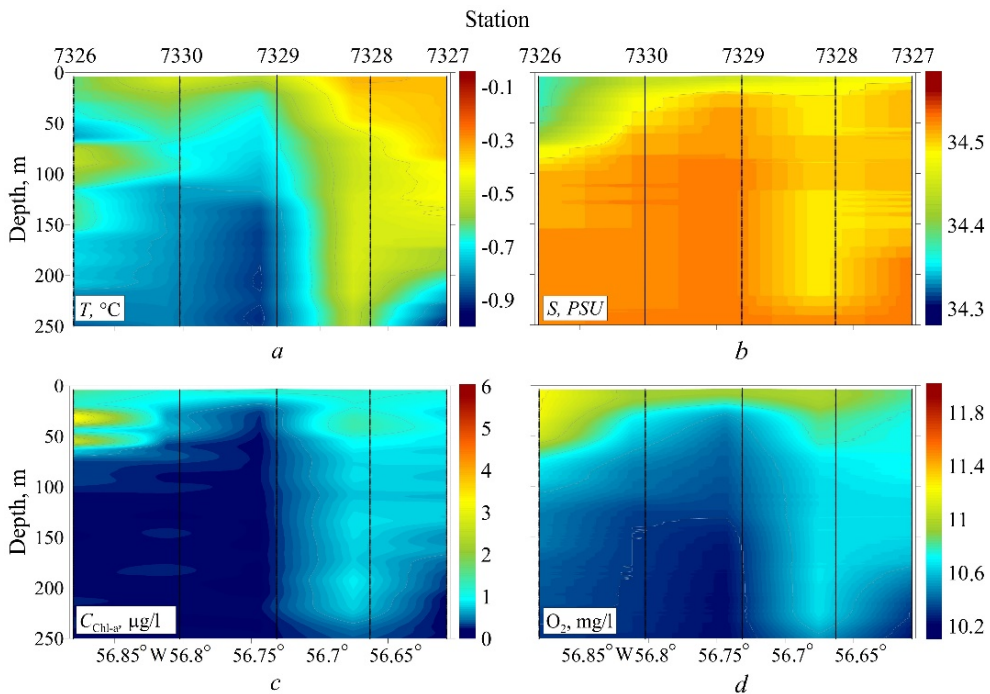


Fig. 3. Cross-sectional vertical section of temperature (a), salinity (b), chlorophyll a (c) and dissolved oxygen (d) concentrations

In the western part of the strait at station 7326 the coldest (Fig. 3, a) waters in the entire layer were recorded, the maximum content of C_{Chl-a} (3.5 $\mu\text{g/l}$) (Fig. 3, c) and O_2 (11.2 mg/l) (Fig. 3, d) – in the upper 70-m layer. On the section in the vicinity of station

7330 and 7329 an upwelling, the rise of cold deep saline waters (Fig. 3, b) with a low content of C_{Chl-a} and O_2 , is well pronounced.

In the eastern part of the strait, near stations 7327 and 7328, a downwelling, as a result of which the warmer and less saline water of the upper layer with high content of O_2 and C_{Chl-a} descends to the lower layers to 320 m, is well developed.

Scatterplots. The characteristic features of water mass distribution in the Antarctic Sound are highlighted in the scatterplots of hydrooptical and hydrological characteristics (Fig. 4).

In T, S (Fig. 4, a) and BAC_{660}, S (Fig. 4, b) diagrams for offshore northern stations 7324 and 7325 (in the upper right part of Fig. 4, a) the warmest and most saline waters of the Bransfield Strait stand out. The salinity of these waters, compared with the temperature and the beam attenuation coefficient at 660 nm, varies slightly with depth, within the range of 34.54–34.56 PSU.

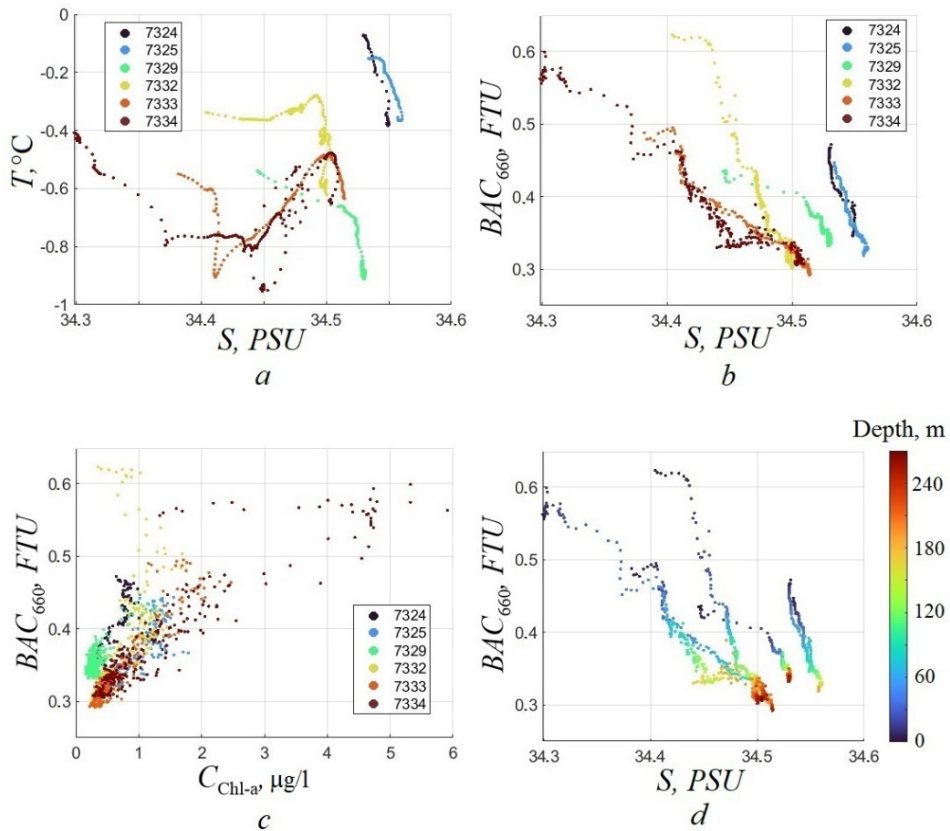


Fig. 4. Scatterplot of temperature and salinity (a), beam attenuation coefficient and salinity (b), beam attenuation coefficient and chlorophyll *a* concentration (c), beam attenuation coefficient and salinity (d) over the entire axial section dataset. The station numbers on graphs a – c and the depth on graph d are highlighted in color

Diagrams T, S and BAC_{660}, S for the southern stations 7333 and 7334 differ from the diagrams for the northern stations in lower temperature and salinity. In the upper

layer of 0–200 m, salinity varies over a much larger range compared to the lower layer waters at the same stations and the waters of the Bransfield Strait at the northern stations. This may be due to the melting of ice in the Weddell Sea during the summer.

An intermediate position on the diagrams is occupied by station 7329, which is located above the top of the seamount in the middle part of the strait at the intersection of the longitudinal and transverse sections. T , S and BAC_{660} , S diagrams for this station are characterized by relatively low temperature, intermediate salinity compared to the northern (7324, 7325) and southern (7333, 7334) stations, as well as increased BAC_{660} values at depths greater than 100 m. The specified station under the upwelling effect in the upper layer contains the water of the underlying layers surrounding the seamount. The water rise and the decrease in the upper layer temperature here are due to a mesoscale cyclonic eddy above the mount, which is manifested in most of the hydrophysical characteristics in the longitudinal and transverse sections (Fig. 2, 3), as well as in T , S and BAC_{660} , S diagrams.

In T , S , BAC_{660} , S and BAC_{660} , C_{Chl-a} diagrams for station 7332 in the upper layer up to 60 m, the values of T and BAC_{660} are higher than for the neighboring station 7333: $T > -0.4^{\circ}\text{C}$ and $BAC_{660} > 0.6$ FTU at station 7332; $T < -0.5^{\circ}\text{C}$ and $BAC_{660} < 0.5$ FTU at station 7333. At the same time, C_{Chl-a} values are lower and amount to 0.1–1 $\mu\text{g/l}$ at station 7332 and 1–2 $\mu\text{g/l}$ at station 7333. Accordingly, the assumption (Fig. 2, *c, e, f*) that the increase in BAC_{660} here is due to the melting of contaminated ice and does not depend on phytoplankton is confirmed. With an increase in the depth, water characteristics at station 7332 approach the characteristics of the Weddell Sea waters at the southern stations of the longitudinal section.

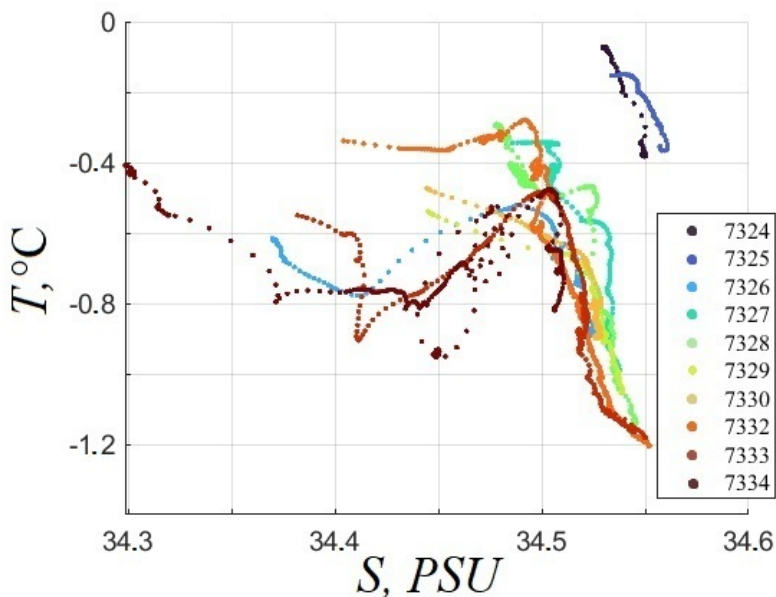


Fig. 5. T - S diagram for the entire dataset

In T, S diagram for all stations performed in the strait (Fig. 5), it can be seen that in the western part of the cross-section, the Weddell Sea waters propagate throughout the entire layer to the bottom. In the eastern part of the section, in the upper layer up to 200 m, the transformed waters, which have intermediate characteristics between the waters of the Weddell Sea and the Bransfield Strait, are formed. The transformation of these waters can be associated with the effect of the system of mesoscale eddies noted earlier in the sections (Fig. 2, 3) and found in satellite images.

Analysis of satellite images. In Fig. 6 and 7, optical and radar satellite images of high spatial resolution are given.

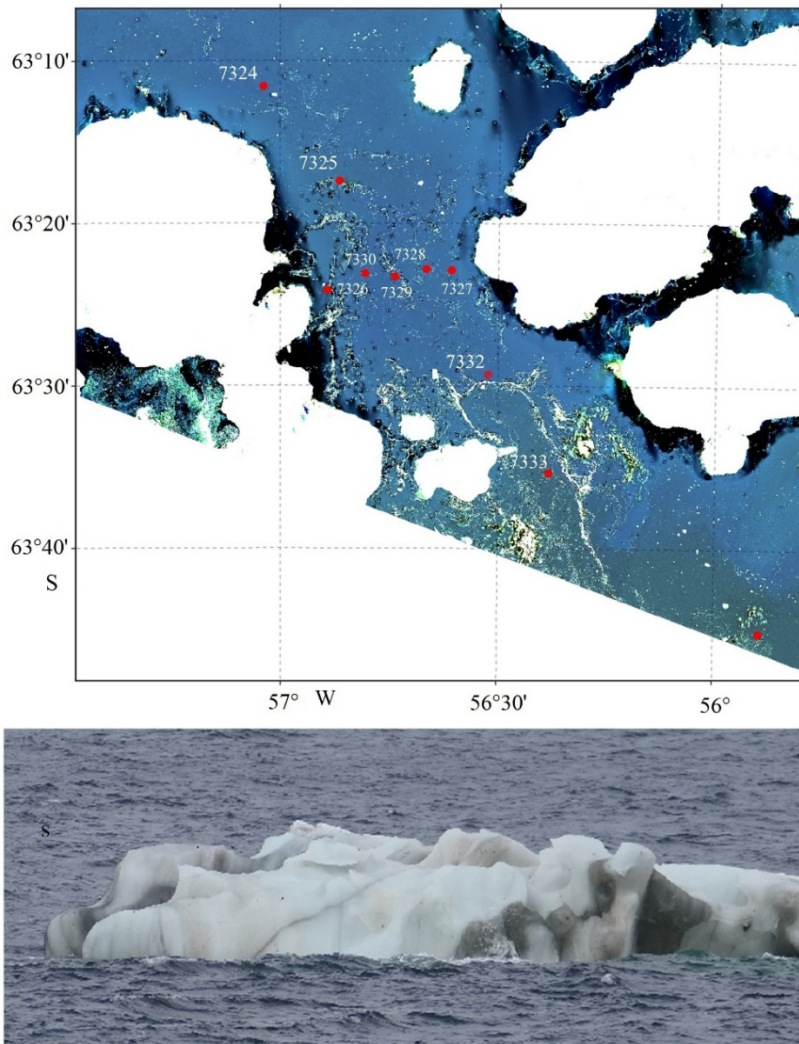


Fig. 6. Satellite RGB-image of the sea surface (Landsat-8) on January 17, 2022 in the southeastern part of the Antarctic Sound and the adjacent area of the western Weddell Sea (above), as well as a photo of the polluted drifting ice in the area of station 7332 (January 28, 2022) (below)

In Fig. 6, the satellite RGB-image reveals the presence of a pronounced mesoscale anticyclonic eddy in the southern part of the Antarctic Sound in the area of stations 7332 and 7333. The eddy appears as a light curve reflecting the inflow of ice fragments and optically active substances brought by them from the Weddell Sea to the southeastern part of the Antarctic Sound basin, where ice is involved in cyclonic circulation. The diameter of the eddy is ~ 8 km.

In Fig. 6 (bottom) an ice fragment that is a component of the light band under consideration is shown. This ice is contaminated with land soil or bottom sediments of a shallow shelf. Its melting leads to an increase in BAC_{660} due to the release of suspended particles into the water that are not associated with phytoplankton communities, which is consistent with the results presented in Fig. 2, *c, e, f* and Fig. 4, *b*.

In Fig. 7, a high-resolution (5–40 m) radar image of the sea surface roughness field in the region of the central part of the Antarctic Sound is demonstrated.

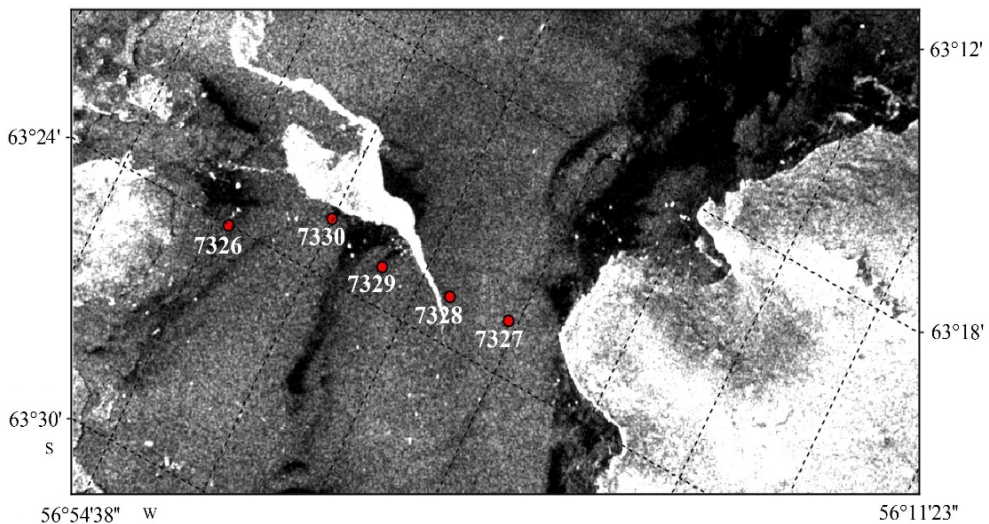


Fig. 7. Fragment of the Sentinel-1 derived high-resolution image (February 19, 2022)

The areas of upwelling and downwelling of waters in all sections are well traced according to the data of ship measurements (Fig. 2, 3). In the satellite radar image (Fig. 7), the upwelling areas on the sections correspond to dark zones with the least roughness of the sea surface on scales of ~ 5.5 m. In the zones of current velocity cyclonic vorticity, both mesoscale [1] and submesoscale cyclonic eddies are generated. They are formed, in particular, on the periphery of mesoscale anticyclones [24]. The alternation of zones of convergence and divergence, downwelling and upwelling, including over the slope and the edge of the Patagonian shelf [25], is a characteristic feature of the mesoscale and submesoscale circulation in the areas of the currents above the slope and edge of the shelf, as well as over the adjacent part of the continental slope.

The zones of current velocity vector convergence in the upper layer of the sea and downwelling, including in mesoscale anticyclonic eddies, correspond to the greater roughness of the sea surface, which is shown by a lighter tone in Fig. 7.

Let us note that on February 19, 2022, the weather was favorable and the wind velocity did not exceed 4 m/s. Therefore, the radar image on that day can be interpreted in the context of our work. On other dates, with a wind exceeding 5 m/s and well-defined wind waves on radar images, it is more difficult to distinguish the zones of convergence, divergence, cyclonic and anticyclonic eddies in the field of sea surface roughness.

Conclusion

Based on the data of hydrooptical and hydrological measurements on January 27–28, 2022, as well as satellite information, obtained during the 87th cruise of R/V “Akademik Mstislav Keldysh”, as well as satellite information, the main features of the mesoscale circulation in the Antarctic Sound within the cyclonic circulation over the deep basin of the southern part of the strait were determined. A joint analysis of the hydrooptical and hydrological characteristics obtained during the Antarctic expedition and satellite measurements in the Antarctic Sound revealed the presence of a system of alternating anticyclonic and cyclonic eddies in the area under study.

This system of mesoscale eddies enhances the exchange between the waters of the upper and deep layers of the strait, as well as between the waters of the Weddell Sea, propagating in the strait towards the north-northwest along the slope of the Antarctic Peninsula bottom, and the waters of the Bransfield Strait, propagating along the slope of the shelf of the islands towards the northeastern boundary of the strait.

It is demonstrated that in the drift areas of the ice contaminated with land soil or shelf bottom sediments, a zone of increased turbidity is formed, which is associated not with phytoplankton blooms, but with the entry of terrigenous suspension into the water during the contaminated ice melting.

REFERENCES

1. Ponomarev, V.I., Fayman, P.A., Prants, S.V., Budyansky, M.V. and Uleysky, M.Yu., 2018. Simulation of Mesoscale Circulation in the Tatar Strait of the Japan Sea. *Ocean Modelling*, 126, pp. 43-55. doi:10.1016/j.ocemod.2018.04.006
2. Jersild, A., Delawalla, S. and Ito, T., 2021. Mesoscale Eddies Regulate Seasonal Iron Supply and Carbon Drawdown in the Drake Passage. *Geophysical Research Letters*, 48(24), e2021GL096020. doi:10.1029/2021GL096020
3. Krek, A.V., Krek, E.V. and Krechik, V.A., 2021. The Circulation and Mixing Zone in the Antarctic Sound in February 2020. In: E. G. Morozov, M. V. Flint and V. A. Spiridonov, 2021. *Antarctic Peninsula Region of the Southern Ocean*. Cham: Springer, pp. 83-99. doi:10.1007/978-3-030-78927-5_6
4. Collares, L.L., Mata, M.M., Kerr, R., Arigony-Neto, J. and Barbat, M.M., 2018. Iceberg Drift and Ocean Circulation in the Northwestern Weddell Sea, Antarctica. *Deep Sea Research Part II: Topical Studies in Oceanography*, 149, pp. 10-24. doi:10.1016/j.dsr2.2018.02.014

5. Thompson, A.F., Heywood, K.J., Thorpe, S.E., Renner, A.H.H. and Trasviña, A., 2009. Surface Circulation at the Tip of the Antarctic Peninsula from Drifters. *Journal of Physical Oceanography*, 39(1), pp. 3-26. doi:10.1175/2008JPO3995.1
6. Van Caspel, M., Hellmer, H.H. and Mata, M.M., 2018. On the Ventilation of Bransfield Strait Deep Basins. *Deep Sea Research Part II: Topical Studies in Oceanography*, 149, pp. 25-30. doi:10.1016/j.dsr2.2017.09.006
7. Gordon, A.L., Mensch, M., Zhaoqian, D., Smethie Jr., W.M. and de Bettencourt, J., 2000. Deep and Bottom Water of the Bransfield Strait Eastern and Central Basins. *Journal of Geophysical Research: Oceans*, 105(C5), pp. 11337-11346. doi:10.1029/2000JC900030
8. Huneke, W.G.C., Huhn, O. and Schröder, M., 2016. Water Masses in the Bransfield Strait and Adjacent Seas, Austral Summer 2013. *Polar Biology*, 39, pp. 789-798. doi:10.1007/s00300-016-1936-8
9. Bograd, S.J., Stabeno, P.J. and Schumacher, J.D., 1994. A Census of Mesoscale Eddies in Shelikof Strait, Alaska, during 1989. *Journal of Geophysical Research: Oceans*, 99(C9), pp. 18243-18254. doi:10.1029/94JC01269
10. Bruce, J.G., 1995. Eddies Southwest of the Denmark Strait. *Deep Sea Research Part I: Oceanographic Research Papers*, 42(1), pp. 13-29. doi:10.1016/0967-0637(94)00040-Y
11. Rabinovich, A.B., Thomson, R.E. and Bograd, S.J., 2002. Drifter Observations of Anticyclonic Eddies near Bussol' Strait, the Kuril Islands. *Journal of Oceanography*, 58, pp. 661-671. doi:10.1023/A:1022890222516
12. Zhou, M., Zhu, Y., Measures, C.I., Hatta, M., Charette, M.A., Gille, S.T., Frants, M., Jiang, M. and Mitchell, B.G., 2013. Winter Mesoscale Circulation on the Shelf Slope Region of the Southern Drake Passage. *Deep-Sea Research Part II: Topical Studies in Oceanography*, 90, pp. 4-14. doi:10.1016/j.dsr2.2013.03.041
13. Bruno, M., Chioua, J., Romero, J., Vázquez, A., Macías, D., Dastis, C., Ramírez-Romero, E., Echevarria, F., Reyes, J. and García, C.M., 2013. The Importance of Sub-Mesoscale Processes for the Exchange of Properties through the Strait of Gibraltar. *Progress in Oceanography*, 116, pp. 66-79. doi:10.1016/j.pcean.2013.06.006
14. Ryan, S., Schröder, M., Huhn, O. and Timmermann, R., 2016. On the Warm Inflow at the Eastern Boundary of the Weddell Gyre. *Deep-Sea Research Part I: Oceanographic Research Papers*, 107, pp. 70-81. doi:10.1016/j.dsr.2015.11.002
15. Vernet, M., Geibert, W., Hoppema, M., Brown, P.J., Haas, C., Hellmer, H.H., Jokat, W., Jullion, L., Mazloff, M. [et al.], 2019. The Weddell Gyre, Southern Ocean: Present Knowledge and Future Challenges. *Reviews of Geophysics*, 57(3), pp. 623-708. doi:10.1029/2018RG000604
16. Nøst, O.A., Biuw, M., Tverberg, V., Lydersen, C., Hattermann, T., Zhou, Q., Smedsrud, L.H. and Kovacs, K.M., 2011. Eddy Overturning of the Antarctic Slope Front Controls Glacial Melting in the Eastern Weddell Sea. *Journal of Geophysical Research: Oceans*, 116(C11), C11014. doi:10.1029/2011JC006965
17. Thompson, A.F., Heywood, K.J., Schmidtke, S. and Stewart, A.L., 2014. Eddy Transport as a Key Component of the Antarctic Overturning Circulation. *Nature Geoscience*, 7, pp. 879-884. doi:10.1038/ngeo2289
18. Stewart, A.L., Klocker, A. and Menemenlis, D., 2018. Circum-Antarctic Shoreward Heat Transport Derived from an Eddy-and Tide-Resolving Simulation. *Geophysical Research Letters*, 45(2), pp. 834-845. doi:10.1002/2017GL075677
19. Jerlov, N.G., 1976. *Marine Optics*. Elsevier Oceanography Series, vol. 14. Amsterdam: Elsevier, 231 p.
20. Chapron, B., Kudryavtsev, V.N., Collard, F., Rasche, N., Kubryakov, A.A. and Stanichny, S.V., 2020. Studies of Sub-Mesoscale Variability of the Ocean Upper Layer Based on Satellite Observations Data. *Physical Oceanography*, 27(6), pp. 619-630. doi:10.22449/1573-160X-2020-6-619-630

21. Kudryavtsev, V.N., Akimov, D.B. and Johannessen, O.M., 2003. Radar Imaging of the Ocean Mesoscale Variability. *Earth Observations from Space*, 2, pp. 27-46 (in Russian).
22. Lavrova, O.Yu., Mityagina, M.I., Sabinin, K.D. and Serebryany, A.N., 2015. Study of Hydrodynamic Processes in the Shelf Zone Based on Satellite Data and Subsatellite Measurements. *Sovremennye Problemy Distantionnogo Zondirovaniya Zemli iz Kosmosa*, 12(5), pp. 98-129 (in Russian).
23. Prants, S.V., Ponomarev, V.I., Budyansky, M.V., Uleysky, M.Yu. and Fayman, P.A., 2015. Lagrangian Analysis of the Vertical Structure of Eddies Simulated in the Japan Basin of the Japan/East Sea. *Ocean Modelling*, 86, pp. 128-140. doi:10.1016/j.ocemod.2014.12.010
24. Ponomarev, V.I., Fayman, P.A., Dubina, V.A. and Mashkina, I.V., 2013. Features of the Synoptic and Sub-Synoptic Scale Sea Water Dynamics over Continental Slope of the Japan Basin and Primorye Shelf. *Sovremennye Problemy Distantionnogo Zondirovaniya Zemli iz Kosmosa*, 10(2), pp. 155-165 (in Russian).
25. Salyuk, P.A., Glukhovets, D.I., Lipinskaya, N.A., Moiseeva, N.A., Churilova, T.Ya., Ponomarev, V.I., Aglova, E.A., Artemiev, V.A., Latushkin, A.A. and Major, A.Yu., 2021. Variability of the Sea Surface Bio-Optical Characteristics in the Region of Falkland Current and Patagonian Shelf. *Sovremennye Problemy Distantionnogo Zondirovaniya Zemli iz Kosmosa*, 18(6), pp. 200-213. doi:10.21046/2070-7401-2021-18-6-200-213 (in Russian).

About the authors:

Aleksandr A. Latushkin, Junior Research Associate, Marine Hydrophysical Institute of RAS (2 Kapitanskaya Str., Sevastopol, 299011, Russian Federation), **SPIN-code: 1239-2858**, **ORCID ID: 0000-0002-3412-7339**, **ResearcherID: U-8871-2019**, sevsalat@gmail.com

Vladimir I. Ponomarev, Leading Research Associate, Laboratory of Experimental Climatology, POI FEB RAS (43 Baltiyskaya Str., Vladivostok, 690041, Russian Federation), Ph.D. (Phys.-Math.), **SPIN-code: 5421-9651**, **ORCID ID: 0000-0002-0501-460X**, **ResearcherID: B-8444-2014**, pavel.salyuk@gmail.com

Pavel A. Salyuk, Head of Laboratory of Satellite Oceanology and Laser Probing, POI FEB RAS (43 Baltiyskaya Str., Vladivostok, 690041, Russian Federation), Ph.D. (Phys.-Math.), **SPIN-code: 1454-3891**, **ORCID ID: 0000-0002-3224-710X**, **ResearcherID: E-8592-2014**, pavel.salyuk@gmail.com

Dmitry I. Frey, Leading Research Associate, Laboratory of Hydrological Processes, Shirshov Institute of Oceanology, Russian Academy of Sciences, (36 Nakhimovskiy Prospect, Moscow, R117997, Russian Federation), Ph.D. (Phys.-Math.), **SPIN-code: 9228-1374**, **ORCID ID: 0000-0001-8141-9513**, **ResearcherID: X-9812-2018**, dima.frey@gmail.com

Nadezhda A. Lipinskaya, Senior Engineer, Laboratory of Experimental Climatology, POI FEB RAS (43 Baltiyskaya Str., Vladivostok, 690041, Russian Federation), **SPIN-code: 2826-5686**, **ORCID ID: 0000-0002-3177-4426**, **ResearcherID: AGE-0831-2022**, ef.na.hc@gmail.com

Svetlana P. Shkorba, Research Associate, Laboratory of Hydrological Processes and Climate, POI FEB RAS (43 Baltiyskaya Str., Vladivostok, 690041, Russian Federation), **SPIN-code: 8197-6065**, **ORCID ID: 0000-0002-2385-7686**, **ResearcherID: B-7713-2014**, podtel@poi.dvo.ru

Contribution of the co-authors:

Aleksandr A. Latushkin – preparation of the paper text, editing the paper text, planning and performing hydrooptical measurements, field data processing, complex data analysis, construction of graphs and distributions

Vladimir I. Ponomarev – formulation of the general research problem, preparation of the paper text, formulation of conclusions

Pavel A. Salyuk – development of methods and conducting experimental studies, discussion of the work results, editing and supplementing of the paper text

Frey D.I. – processing and analysis of hydrophysical data

Nadezhda A. Lipinskaya – visualization/presentation of data in the text, computer work, satellite imaging

Svetlana P. Shkorba – selection and analysis of literature, collection of radar data, editing the text of the paper

The authors have read and approved the final manuscript.

The authors declare that they have no conflict of interest.